

Glino Pair Production at Linear e^+e^- Colliders

Stefan Berge and Michael Klasen*

*II. Institut für Theoretische Physik, Universität Hamburg,
Luruper Chaussee 149, D-22761 Hamburg, Germany*

(Dated: October 28, 2018)

Abstract

We study the potential of high-energy linear e^+e^- colliders for the production of gluino pairs within the Minimal Supersymmetric Standard Model (MSSM). In this model, the process $e^+e^- \rightarrow \tilde{g}\tilde{g}$ is mediated by quark/squark loops, dominantly of the third generation, where the mixing of left- and right-handed states can become large. Taking into account realistic beam polarization effects, photon and Z^0 -boson exchange, and current mass exclusion limits, we scan the MSSM parameter space for various e^+e^- center-of-mass energies to determine the regions, where gluino production should be visible.

arXiv:hep-ph/0208212v1 23 Aug 2002

*michael.klasen@desy.de

I. INTRODUCTION

Supersymmetry (SUSY) is generally considered to be one of the most promising extensions of the Standard Model (SM) of particle physics. Its attractive features include the cancellation of quadratic divergences in the Higgs sector, which implies that the soft SUSY breaking masses of the (yet unobserved) superpartners of the SM particles can not be much greater than the electroweak scale. If SUSY is indeed responsible for the stabilization of this scale against the Planck scale, supersymmetric particles should therefore be discovered either at Run II of the Fermilab Tevatron [1, 2, 3, 4, 5] or at the CERN LHC [6, 7]. In particular, the strongly coupling squarks and gluinos should be copiously produced at hadron colliders and lead to first measurements of their masses and production cross sections [8]. Precision measurements of masses, mixings, quantum numbers, and couplings must, however, be performed in the clean environment of a future linear e^+e^- collider because of the large hadronic SM background and theoretical scale and parton density uncertainties at the Fermilab Tevatron and CERN LHC. For example, in e^+e^- annihilation the center-of-mass energy of the collision is exactly known, and threshold energy scans allow for a precise mass determination of pair-produced SUSY particles. It will then be possible to establish whether the masses and couplings of the electroweak gauginos and of the gluino are indeed related, as expected. A global analysis should ultimately lead to a reconstruction of the SUSY breaking model and its parameters. Along these lines, detailed studies have recently been performed for squarks, sleptons, charginos, and neutralinos [9], but not for gluinos, the reason being that gluino pairs are produced at e^+e^- colliders only at the one-loop level, while all other sparticles are produced at tree level. At tree level, gluinos can be produced in pairs only in association with two quarks [10], or they are produced singly in association with a quark and a squark [11, 12]. Both processes result in multi-jet final states, where phase space is limited and gluinos may be hard to isolate.

In the Minimal Supersymmetric Standard Model (MSSM) [13, 14], the exclusive production of gluino pairs in e^+e^- annihilation is mediated by s -channel photons and Z^0 -bosons, which couple to the gluinos via triangular quark and squark loops. In earlier studies of this process only the very low center-of-mass energy region ($\sqrt{s} = 20$ GeV) with pure photon exchange and no squark mixing [15] or Z^0 -boson decays into light ($m_{\tilde{g}} < m_Z/2$) [16, 17] and very light ($m_{\tilde{g}} = 3 \dots 5$ GeV) [18, 19] gluinos have been considered. Some authors have

presented results only for $m_{\tilde{g}} = 0$ GeV and outdated top quark masses of 20...50 GeV [16, 19], while others have neglected the mixing of left- and right-handed squark interaction eigenstates into light and heavy mass eigenstates [15, 16, 17], which turns out to control the production cross section to a large extent.

It is the aim of this Article to study the potential of high-energy linear e^+e^- colliders for the production of gluino pairs within the MSSM. Taking into account realistic beam polarization effects, photon and Z^0 -boson exchange, and current mass exclusion limits, we scan the MSSM parameter space for various e^+e^- center-of-mass energies to determine the regions, where gluino production should be visible. Furthermore we clarify the theoretical questions of the relative sign between the two contributing triangular Feynman diagrams, of the possible presence of an axial vector anomaly, and the conditions for vanishing cross sections – three related issues, which have so far been under debate in the literature. The remainder of this Paper is organized as follows: In Sec. II, we present our analytical results and compare them with existing results in the literature. Various numerical cross-sections for gluino pair production at future high-energy linear e^+e^- colliders are computed and discussed in Sec. III, and Sec. IV contains our Conclusions. Our conventions for squark mixing are defined in App. A, and a summary of all relevant Feynman rules is given in App. B.

II. ANALYTICAL RESULTS

The scattering process

$$e^-(p_1, \lambda_1)e^+(p_2, \lambda_2) \rightarrow \tilde{g}(k_1)\tilde{g}(k_2) \quad (1)$$

with incoming electron/positron momenta $p_{1,2}$ and helicities $\lambda_{1,2}$ and outgoing gluino momenta $k_{1,2}$ proceeds through the two Feynman diagrams A and B in Fig. 1 with s -channel photon and Z^0 -boson exchange and triangular quark and squark loops. Higgs boson exchange is not considered due to the negligibly small electron Yukawa coupling, but it could well be relevant at muon colliders. The process occurs only at the one-loop level, since the gluino as the superpartner of the gauge boson of the strong interaction couples neither directly to leptons nor to electroweak gauge bosons. Taking into account chiral squark mixing (see App. A) and using the Feynman rules in App. B, we decompose the corresponding

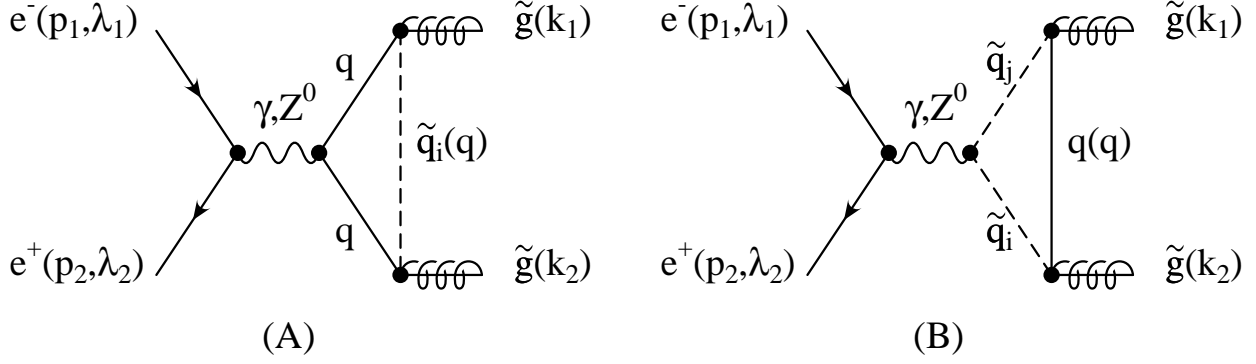


FIG. 1: Feynman diagrams for gluino pair production in electron-positron annihilation. The exchanged photons and Z^0 -bosons couple to the produced gluinos through triangular $qq\tilde{q}_i$ (A) and $\tilde{q}_i\tilde{q}_j q$ (B) loops with flavor flow in both directions.

scattering amplitude

$$\mathcal{M} = \sum_{V=\gamma, Z^0} L_\mu^V iD_V^{\mu\nu} G_\nu^V \quad (2)$$

into the lepton current

$$L_\mu^V = \bar{v}(p_2, \lambda_2) \left[-ie\gamma_\mu (v_e^V - a_e^V \gamma_5) \right] u(p_1, \lambda_1), \quad (3)$$

the photon and Z^0 -boson propagators

$$iD_V^{\mu\nu} = \frac{-ig^{\mu\nu}}{s - m_V^2 + i\eta}, \quad V = \gamma, Z^0, \quad (4)$$

which depend on the squared center-of-mass energy $s = (p_1 + p_2)^2$, and the gluino current

$$G_\nu^V = -e\bar{u}(k_2) \sum_q \left[\sum_i \left(i\Gamma_{i,1}^a A_\nu^{i,V} i\Gamma_{i,2}^b + i\Gamma_{i,2}^a \tilde{A}_\nu^{i,V} i\Gamma_{i,1}^b \right) \right. \\ \left. + \sum_{i,j} \left(i\Gamma_{i,1}^a \Gamma_q^{ij,V} B_\nu^{ij,V} i\Gamma_{j,2}^b + i\Gamma_{i,2}^a \Gamma_q^{ji,V} \tilde{B}_\nu^{ij,V} i\Gamma_{j,1}^b \right) \right] v(k_1) \quad (5)$$

with squark mass eigenstates $i, j = \{1, 2\}$,

$$A_\nu^{i,V} = \int \frac{d^D q}{(2\pi)^D} \mu^{4-D} \frac{(\not{q} + \not{k}_2 + m_q)\gamma_\nu (v_q^V - a_q^V \gamma_5)(\not{q} - \not{k}_1 + m_q)}{(q^2 - m_i^2 + i\eta)[(q - k_1)^2 - m_q^2 + i\eta][(q + k_2)^2 - m_q^2 + i\eta]} \quad (6)$$

and

$$B_\nu^{ij,V} = \int \frac{d^D q}{(2\pi)^D} \mu^{4-D} \frac{(\not{q} - m_q)(2q - k_1 + k_2)_\nu}{(q^2 - m_q^2 + i\eta)[(q - k_1)^2 - m_j^2 + i\eta][(q + k_2)^2 - m_i^2 + i\eta]} \quad (7)$$

and the quark flavor q flowing both ways in the corresponding diagrams A and B, so that $\tilde{A}_\nu^{i,V} = A_\nu^{i,V}(v_q^V \rightarrow -v_q^V)$, $\tilde{B}_\nu^{ij,V} = -B_\nu^{ij,V}$, and $\Gamma' = C\Gamma^T C^{-1} = \Gamma$ [20].

Eq. (5) can be simplified with the Dirac equation and the anti-commutation relations for Dirac matrices, and the tensor loop integrals in Eqs. (6) and (7) can be expressed through the standard coefficient functions $C_{k(l)}$ of the metric tensor $g_{\mu\nu}$ and tensors constructed from the outgoing gluino momenta $k_{1,\mu}$ and $k_{2,\mu}$ [20, 21]. The gluino current then reduces to

$$G_\nu^V = ie \frac{\alpha_s}{2\pi} \frac{\delta^{ab}}{2} \bar{u}(k_2) \gamma_\nu \gamma_5 v(k_1) \sum_q (A_q^V + B_q^V) \quad (8)$$

with

$$\begin{aligned} A_q^V &= \sum_i \left[C_0^{qi} (m_q^2 a_{qiV}^- - m_{\tilde{g}}^2 a_{qiV}^+ + 2m_q m_{\tilde{g}} \hat{a}_{qiV}) + C_1^{qi} 4m_{\tilde{g}} (m_q \hat{a}_{qiV} - m_{\tilde{g}} a_{qiV}^+) \right. \\ &\quad \left. + C_{00}^{qi} (2 - D) a_{qiV}^+ - C_{11}^{qi} 2m_{\tilde{g}}^2 a_{qiV}^+ + C_{12}^{qi} (s - 2m_{\tilde{g}}^2) a_{qiV}^+ \right], \\ B_q^V &= \sum_{i,j} C_{00}^{qij} 2b_{qijV}, \end{aligned} \quad (9)$$

$$(10)$$

where $C_{k(l)}^{qi} = C_{k(l)}(m_{\tilde{g}}^2, s, m_{\tilde{g}}^2, m_{\tilde{q}_i}^2, m_q^2, m_q^2)$ and $C_{00}^{qij} = C_{00}(m_{\tilde{g}}^2, s, m_{\tilde{g}}^2, m_q^2, m_{\tilde{q}_j}^2, m_{\tilde{q}_i}^2)$ are massive (infrared-finite) three-point functions and $C_1^{qi} = C_2^{qi}$ and $C_{11}^{qi} = C_{22}^{qi}$ in diagram A.

$$\begin{aligned} a_{qiV}^\pm &= v_q^V (S_{i1}^q S_{i1}^{q*} - S_{i2}^q S_{i2}^{q*}) \pm a_q^V, \\ \hat{a}_{qiV} &= a_q^V (S_{i1}^q S_{i2}^{q*} + S_{i2}^q S_{i1}^{q*}), \text{ and} \\ b_{qijV} &= S_{i1}^q S_{j1}^{q*} \Gamma_q^{ij,V} - S_{i2}^{q*} S_{j2}^q \Gamma_q^{ji,V} \end{aligned} \quad (11)$$

are combinations of vector (v_q^V), axial vector (a_q^V), and derivative couplings ($\Gamma_q^{ij,V}$), and elements of the squark mixing matrix S . Pairs of identical (Majorana) gluinos are therefore produced by a parity violating axial vector coupling induced by mass differences between the chiral squarks and the axial vector coupling a_q^Z of the Z^0 -boson. The (mass-independent) ultraviolet singularities contained in the C_{00} -functions cancel among A_q^V and B_q^V in $D = 4 - 2\epsilon$ dimensions. As we have checked explicitly (even for complex squark mixing matrices), adding the two amplitudes induces not only a cancellation of the ultraviolet singularities and of the logarithmic dependence on the scale parameter μ introduced in Eqs. (6) and (7) in order to preserve the mass dimension of the loop integrals, but also a destructive interference of the finite remainders. This happens separately for each weak isospin partner, as is to be expected for triangular loop diagrams involving one axial vector and two scalar (not vector) couplings and no closed fermion loop.

The (finite) total cross section for incoming electrons/positrons with helicities $\lambda_{1,2} = \pm 1/2$ is then

$$\sigma_{\lambda_1\lambda_2}(s) = \frac{\alpha_e^2 \alpha_s^2 (N_C^2 - 1) \beta^3 s}{24\pi} \sum_{V_1, V_2} \left[\frac{Q_{\lambda_1\lambda_2}^{V_1 V_2}}{(s - m_{V_1}^2)(s - m_{V_2}^2)} \sum_q (A_q^{V_1} + B_q^{V_1})(A_q^{V_2} + B_q^{V_2})^* \right] \quad (12)$$

with

$$Q_{\lambda_1\lambda_2}^{V_1 V_2} = (v_e^{V_1} v_e^{V_2} + a_e^{V_1} a_e^{V_2})(1 - 4\lambda_1\lambda_2) - (v_e^{V_1} a_e^{V_2} + v_e^{V_2} a_e^{V_1})(2\lambda_1 - 2\lambda_2), \quad (13)$$

color factor $N_C = 3$, and gluino velocity $\beta = \sqrt{1 - 4m_g^2/s}$, which contains the expected factors of β^3 and s for P -wave production of two spin-1/2 Majorana fermions. The distribution in the center-of-mass scattering angle θ ,

$$\frac{d\sigma_{\lambda_1\lambda_2}}{d\Omega}(s) = \frac{3}{8\pi}(1 + \cos^2\theta)\sigma_{\lambda_1\lambda_2}(s), \quad (14)$$

is independent of the gluino mass and has to be integrated over just one hemisphere, since the two final state particles are identical [18, 22]. As a consequence, the forward-backward asymmetry vanishes for Majorana fermions, but not for Dirac fermions.

Our result for diagram A agrees with the unpolarized result

$$\sigma(s) = \frac{1}{4} \sum_{\lambda_{1,2}=\pm 1/2} \sigma_{\lambda_1\lambda_2}(s) \quad (15)$$

in Eq. (4.5) of Kileng and Osland, if we identify [18, 23]

$$\begin{aligned} C_0^{qi} &= -F_{qqi}^{00}, \\ C_1^{qi} &= +F_{qqi}^{01}, \\ C_{00}^{qi} &= -G_{qqi}/2, \\ C_{11}^{qi} &= -F_{qqi}^{02}, \\ C_{12}^{qi} &= -F_{qqi}^{11}, \end{aligned} \quad (16)$$

and reverse the sign of \hat{b}_q to account for opposite conventions of squark mass eigenstates. However, our result for diagram B disagrees in sign with Eq. (4.5) of Kileng and Osland, if we identify [18, 23]

$$C_{00}^{qij} = -G_{ijq}/2. \quad (17)$$

If the sign of diagram B is reversed, the ultraviolet singularities cancel only after adding the contributions from the two weak isospin partners with opposite values of T_q^3 . We trace this

sign discrepancy to the Feynman rules employed in Ref. [18], which exhibit a relative minus sign to those in Ref. [14] for the Z^0 -boson coupling to quarks, but not to squarks, whereas our Feynman rules (see App. B) agree with those in Ref. [14] in the limit of no squark mixing. Except for the relative sign of diagrams A and B and in the limit of vanishing gluino mass, we also find agreement with Djouadi and Drees [19]. We confirm, however, the relative sign for diagrams A and B of Campbell, Scott, and Sundaresan [17], who found (for non-mixing chiral squarks of different mass) that the ultraviolet singularities cancel separately for each weak isospin partner, and that there is no anomaly. This had also been claimed previously by Kane and Rolnick [16] for chiral squarks of equal mass. In their limit, the cross section depends only on the weak isospin and not on the charge of the (s)quarks [16], and the contribution of the photon vanishes [15]. For the contribution of the Z^0 -boson to vanish, we must have [18]

1. mass degeneracy in each quark isospin doublet, $m_d = m_u$ etc.,
2. mass degeneracy in each squark isospin doublet, $m_{\bar{d}_1} = m_{\bar{d}_2} = m_{\bar{u}_1} = m_{\bar{u}_2}$ etc.,

which contradicts the condition $m_q = m_{\bar{q}}$ found by Kane and Rolnick [16]. Condition (1) is violated most strongly for the third generation, as is condition (2) for most SUSY breaking models.

III. NUMERICAL RESULTS

The analytical results presented in the previous Section have been obtained in two independent analytical calculations. They have been implemented in compact Fortran computer codes, which depend on the LoopTools/FF library [24, 25] for the evaluation of the massive tensor three-point functions. As a third independent cross-check, we have recalculated the production of gluino pairs in e^+e^- annihilation with the computer algebra program FeynArts/FormCalc [26] and found numerical agreement up to 15 digits.

Our calculations involve various masses and couplings of SM particles, for which we use the most up-to-date values from the 2002 Review of the Particle Data Group [27]. In particular, we evaluate the electromagnetic fine structure constant $\alpha(m_Z) = 1/127.934$ at the mass of the Z^0 -boson, $m_Z = 91.1876$ GeV, and calculate the weak mixing angle θ_W from the tree-level expression $\sin^2 \theta_W = 1 - m_W^2/m_Z^2$ with $m_W = 80.423$ GeV. Among the

fermion masses, only the one of the top quark, $m_t = 174.3$ GeV, plays a significant role due to its large splitting from the bottom quark mass, $m_b = 4.7$ GeV, while the latter and the charm quark mass, $m_c = 1.5$ GeV, could have been neglected like those of the three light quarks and of the electron/positron. The strong coupling constant is evaluated at the gluino mass scale from the one-loop expression with five active flavors and $\Lambda_{\text{LO}}^{n_f=5} = 83.76$ MeV, corresponding to $\alpha_s(m_Z) = 0.1172$. A variation of the renormalization scale by a factor of four about the gluino mass results in a cross section uncertainty of about $\pm 25\%$. Like the heavy top quark, all SUSY particles have been decoupled from the running of the strong coupling constant.

We work in the framework of the MSSM with conserved R - (matter-) parity, which represents the simplest phenomenologically viable model, but which is still sufficiently general to not depend on a specific SUSY breaking mechanism. Models with broken R -parity are severely restricted by the non-observation of proton decay, which would violate both baryon and lepton number conservation. We do not consider light gluino mass windows, on which the literature has focused so far and which may or may not be excluded from searches at fixed target and collider experiments [27]. Instead, we adopt the current mass limit $m_{\tilde{g}} \geq 200$ GeV from the CDF [28] and D0 [29] searches in the jets with missing energy channel, relevant for non-mixing squark masses of $m_{\tilde{q}} \geq 325$ GeV and $\tan\beta = 3$. Values for the ratio of the Higgs vacuum expectation values, $\tan\beta$, below 2.4 are already excluded by the CERN LEP experiments [30]. If not stated otherwise, we will present unpolarized cross sections for a $\sqrt{s} = 500$ GeV linear e^+e^- collider like DESY TESLA, gluino masses of $m_{\tilde{g}} = 200$ GeV, and squark masses $m_{\tilde{q}} \simeq m_{\tilde{Q}} = m_{\tilde{D}} = m_{\tilde{U}} = m_{\tilde{S}} = m_{\tilde{C}} = m_{\tilde{B}} = m_{\tilde{T}} = m_{\text{SUSY}} = 325$ GeV. We will consider two cases of large squark mass splittings: I.) On the one hand, the masses of the superpartners of left- and right-handed quarks need not be equal to each other. In this scenario we will vary the right-handed up-type squark mass parameters $m_{\tilde{U},\tilde{C},\tilde{T}}$ between 200 and 1500 GeV. II.) On the other hand, the superpartners of the heavy quarks can mix into light and heavy mass eigenstates (see App. A). This alternative is restricted by the CERN LEP limits on the light top and bottom squark masses, $m_{\tilde{t}_1} \geq 100$ GeV and $m_{\tilde{b}_1} \geq 99$ GeV [31], and on SUSY one-loop contributions [32, 33, 34] to the ρ -parameter, $\rho_{\text{SUSY}} < 0.0012$ [27]. In this case we assume the maximally allowed top squark mixing with $\theta_{\tilde{t}} = 45.2^\circ$, $m_{\tilde{t}_1} = 110$ GeV, and $m_{\tilde{t}_2} = 506$ GeV, which can be generated by choosing appropriate values for the Higgs mass parameter, $\mu = -500$ GeV, and the trilinear top squark coupling,

$A_t = 534$ GeV. For small values of $\tan\beta$, mixing in the bottom squark sector remains small, and we take $\theta_{\tilde{b}} = 0^\circ$. Although the absolute magnitude of the cross section depends strongly on the gluino mass and collider energy, the relative importance of the different contributions is very similar also for higher gluino masses and collider energies.

First we examine the conditions found in Section II for vanishing of the photon and Z^0 -boson contributions, restricting ourselves to the third generation. Since we expect the photon contribution to cancel for equal left- and right-handed squark masses, we vary the right-handed top squark mass parameter, $m_{\tilde{T}} \simeq m_{\tilde{t}_R}$, between 200 and 1500 GeV, but keep $m_{\tilde{t}_L} \simeq m_{\tilde{Q}} = m_{\tilde{B}} = m_{\text{SUSY}} = 325$ GeV fixed (case I), since top and bottom squarks generally interfere destructively due to their opposite charge and weak isospin quantum numbers. As can be seen from Fig. 2, the photon contribution cancels indeed for $m_{\tilde{T}} \simeq m_{\tilde{t}_R} = m_{\tilde{t}_L} \simeq m_{\text{SUSY}}$. This is due to the fact that for photons $\hat{a}_{qi\gamma} = 0$ and $b_{q12\gamma} = b_{q21\gamma} = 0$ in Eq. (11), while unitarity of the squark mixing matrix leads to $a_{q1\gamma}^\pm = -a_{q2\gamma}^\pm$ and $b_{q11\gamma} = -b_{q22\gamma}$. Therefore, the photon contributions cancel for all flavors q with equal squark masses. Due to their charge, top (s)quarks contribute four times as much as bottom (s)quarks, whose contribution is even more suppressed by the condition $m_{\tilde{b}_L} \simeq m_{\tilde{b}_R}$. The Z^0 -boson contribution can never cancel, since $m_t \gg m_b$, and therefore it depends only weakly on $m_{\tilde{T}}$, but it can become minimal for $m_{\tilde{T}} \simeq m_{\tilde{t}_R} = m_{\tilde{t}_L} = m_{\tilde{b}_R} = m_{\tilde{b}_L} \simeq m_{\text{SUSY}}$. As $m_{\tilde{T}}$ gets significantly larger (or smaller) than m_{SUSY} , the photon contribution starts to dominate over the Z^0 -boson contribution.

If only $m_{\tilde{T}}$ differs from m_{SUSY} , the third generation contributes almost 100% to the total cross section. However, if $m_{\tilde{U}} = m_{\tilde{C}} = m_{\tilde{T}}$ are varied simultaneously, all three generations contribute to the total cross section, which can therefore become significantly larger. This is shown in Fig. 3, where (s)quark loop contributions from all three generations have been taken into account.

When $m_{\tilde{U}} = m_{\tilde{C}} = m_{\tilde{T}} = m_{\text{SUSY}}$ and large mass splittings are generated only by mixing in the top squark sector (case II), photon contributions are suppressed by more than two orders of magnitude. Fig. 4 shows that the Z^0 -boson contributions from top and bottom squarks interfere destructively due to opposite values of their weak isospin quantum numbers, except for $\theta_{\tilde{t}} \simeq 45.2^\circ$, where the imaginary parts of the amplitudes interfere constructively. It is therefore advantageous to keep the bottom squark mass splitting small. As is also evident from Fig. 4, mixing in the bottom squark sector is of little importance. Note that the central

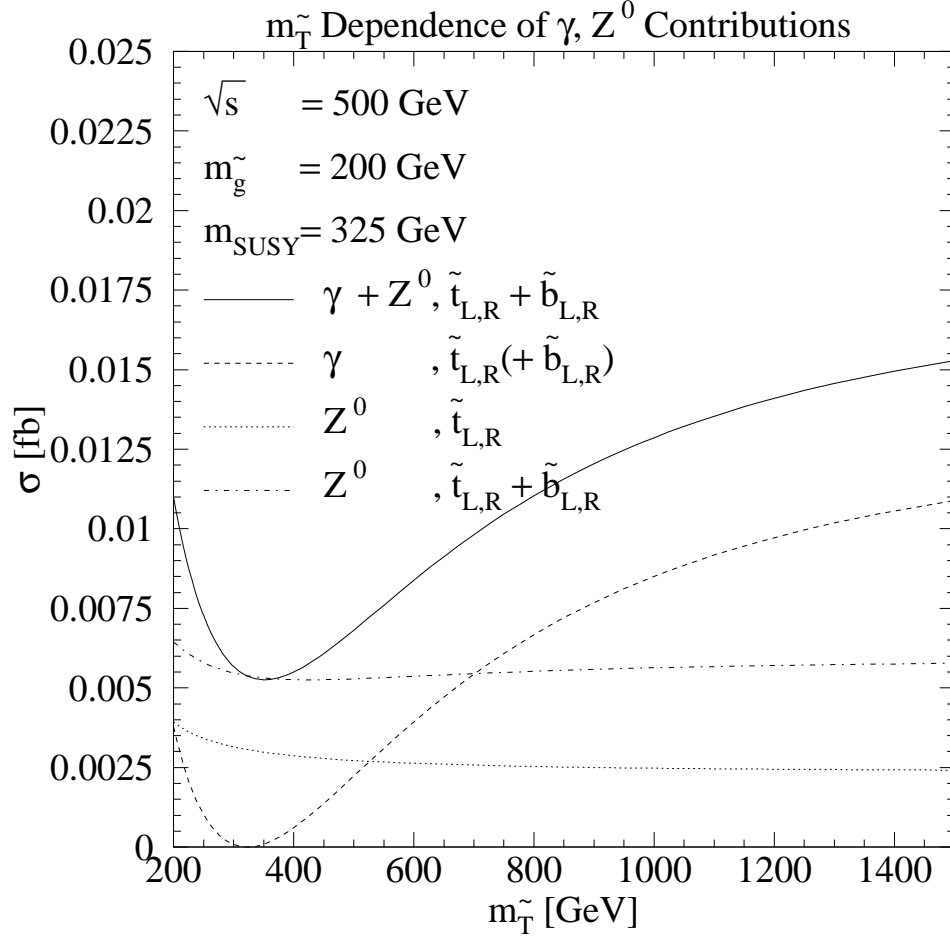


FIG. 2: Dependence of the photon and Z^0 -boson contributions to the process $e^+e^- \rightarrow \tilde{g}\tilde{g}$ on the right-handed top squark mass parameter $m_{\tilde{T}}$. The photon contribution (dashed curve) is dominated by top (s)quarks and cancels for $m_{\tilde{t}_L} = m_{\tilde{t}_R}$. The Z^0 -boson contribution from top (dotted curve) and bottom squarks (dot-dashed curve) interferes constructively with the photon contribution (full curve).

region with maximal top/bottom squark mixing is excluded by the CERN LEP limits on $m_{\tilde{t}_1}$, $m_{\tilde{b}_1}$, and the ρ -parameter.

When m_{SUSY} and the diagonal elements of the squark mixing matrix (see App. A) become much larger than the quark masses and the off-diagonal elements of the matrix, the role of squark mixing is expected to be reduced. This is confirmed numerically in Fig. 5, where the dependence of the gluino production cross section on m_{SUSY} is shown for the cases of maximal and vanishing top squark mixing. Squarks from the first two generations contribute

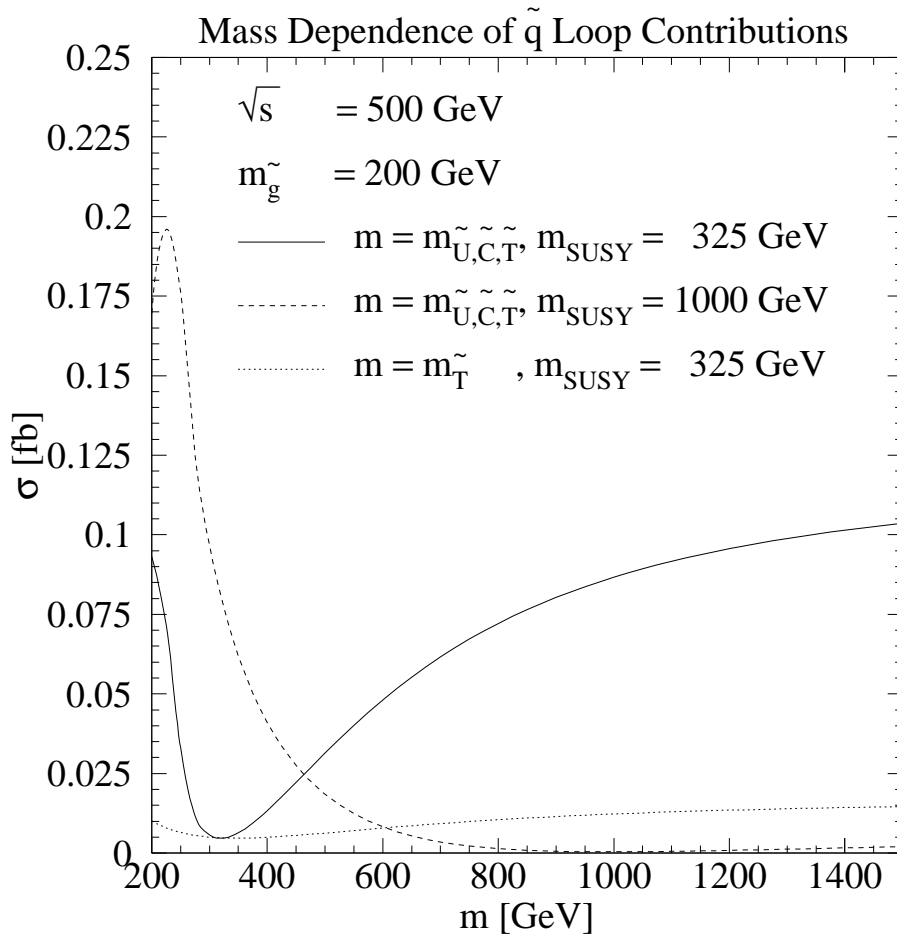


FIG. 3: Dependence of the \tilde{q} loop contributions to the process $e^+e^- \rightarrow \tilde{g}\tilde{g}$ on the right-handed up-type squark mass parameter $m_{\tilde{U}} = m_{\tilde{C}} = m_{\tilde{T}}$. When these mass parameters differ simultaneously from $m_{\text{SUSY}} = 325$ GeV (full curve) or $m_{\text{SUSY}} = 1000$ GeV (dashed curve), all three (s)quark generations contribute significantly to the total cross section, so that it becomes much larger than in the case where only $m_{\tilde{T}}$ is varied (dotted curve).

at most 10% at low m_{SUSY} and are otherwise strongly suppressed.

At future linear e^+e^- colliders it will be possible to obtain relatively high degrees of polarization, *i.e.* about 80% for electrons and 60% for positrons [9]. In Fig. 6 we therefore investigate the effect of choosing different electron/positron polarizations on the gluino pair production process, including contributions from all (s)quarks. Since the $++$ and $--$ helicity amplitudes vanish for both photons and Z^0 -bosons, we only show the squares of the remaining $+-$ and $-+$ amplitudes, which coincide for photons, but not for Z^0 -bosons.

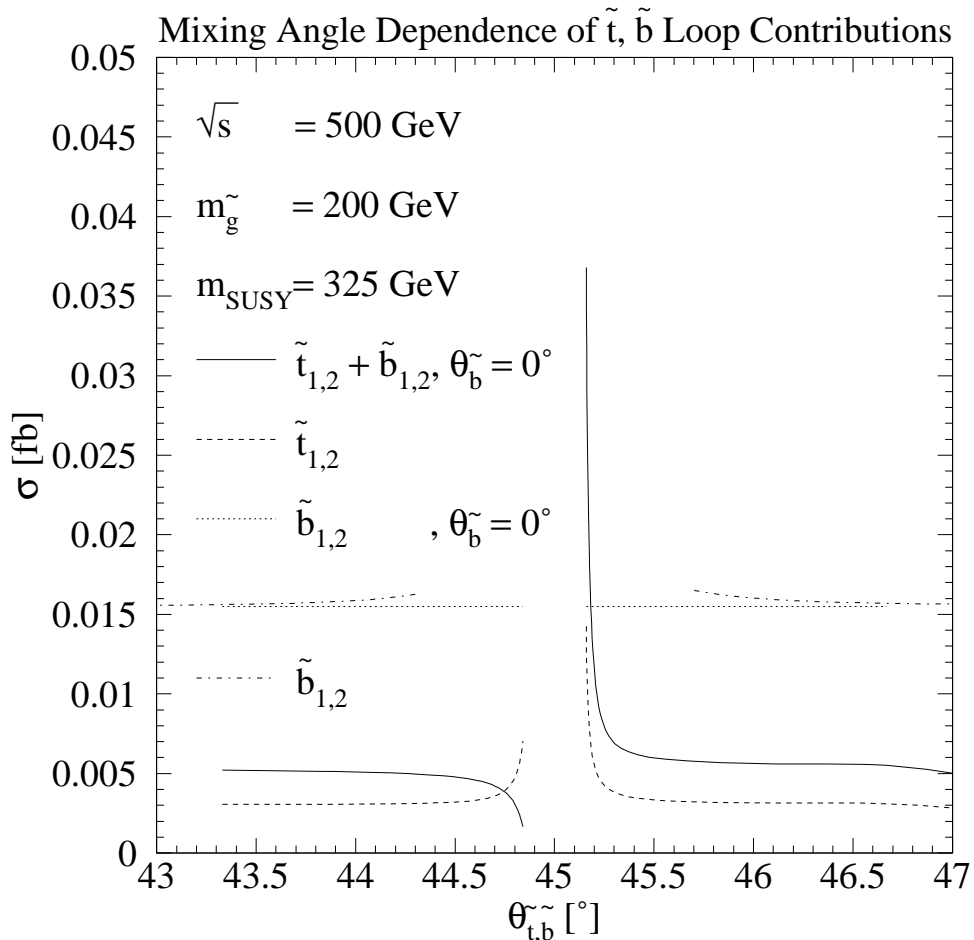


FIG. 4: Mixing angle dependence of the \tilde{t} (dashed) and \tilde{b} (dotted) loop contributions to the process $e^+e^- \rightarrow \tilde{g}\tilde{g}$, which interfere destructively (full curve), except for $\theta_{\tilde{t}} \simeq 45.2^\circ$, where the imaginary parts of the amplitudes interfere constructively. Mixing in the \tilde{b} sector (dot-dashed curve) enhances the cross section only slightly.

The unpolarized cross section falls short of the polarized ones, so that a high degree of polarization is clearly desirable.

With the realistic degrees of polarization mentioned above, we show in Fig. 7 a scan in the center-of-mass energy of a future e^+e^- collider for various gluino masses and maximal top squark mixing (case II). The cross section rises rather slowly due to the factor β^3 in Eq. (12) for P -wave production of the gluino pairs. For $m_{\tilde{g}} = 200$ GeV we observe an interesting second maximum, which arises from the intermediate squark pair resonance at $\sqrt{s} = 2m_{\text{SUSY}} = 650$ GeV. At threshold, the cross section depends strongly on the gluino

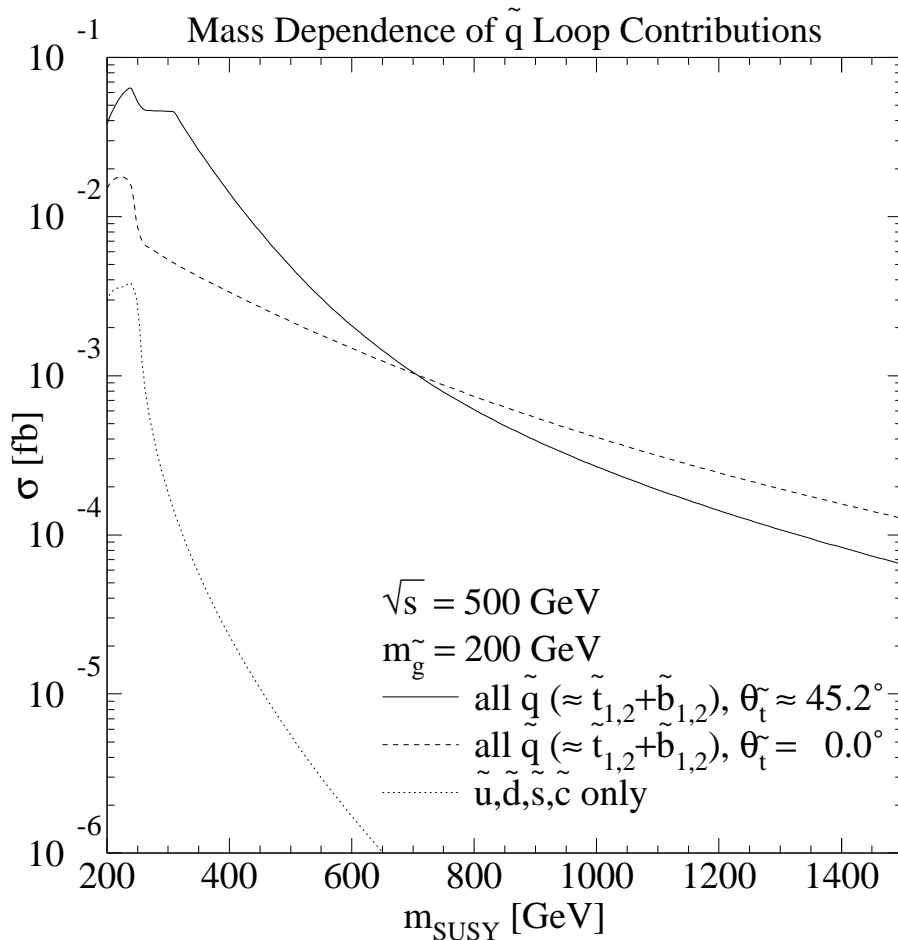


FIG. 5: Squark mass dependence of the loop contributions from third generation squarks with maximal (full curve) and vanishing mixing (dashed curve). The contributions from the first two generations (dotted curve) are highly suppressed.

mass and is largest for $m_{\tilde{g}} = 200 \text{ GeV}$, which we consider to be the lowest experimentally allowed value. It drops fast with $m_{\tilde{g}}$, so that for $m_{\tilde{g}} > 500 \text{ GeV}$ no events at colliders with luminosities of 1000 fb^{-1} per year can be expected, irrespective of their energy. Smaller squark mixing (cf. Fig. 4) or larger values of m_{SUSY} (cf. Fig. 5) will reduce the cross section even further. Far above threshold, it drops off like $1/s$ and becomes independent of the gluino mass.

The slow rise of the cross section can be observed even better in Fig. 8, where the sensitivity of a $\sqrt{s} = 500 \text{ GeV}$ collider like DESY TESLA to gluino masses around 200 GeV has been plotted. For the CERN LHC experiments, a precision of $\pm 30 \dots 60$ ($12 \dots 25$) GeV

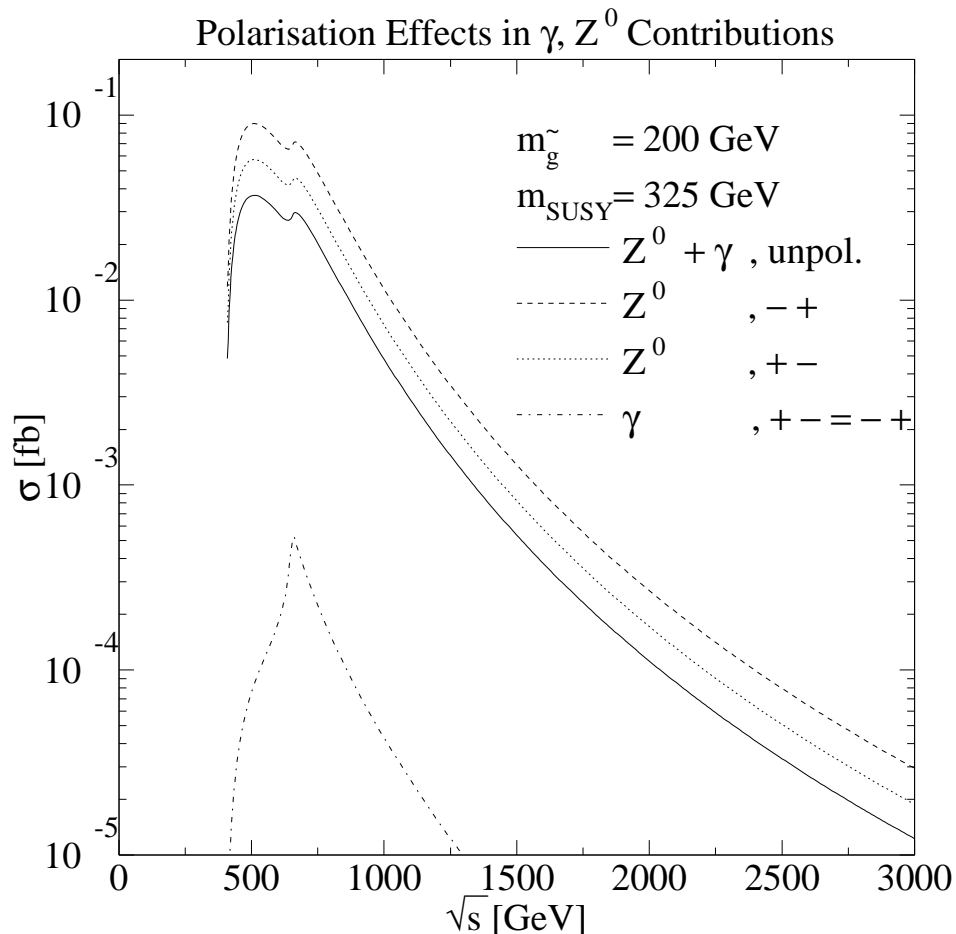


FIG. 6: Center-of-mass energy dependence of the process $e^+e^- \rightarrow \tilde{g}\tilde{g}$ for unpolarized (full curve) and polarized (dashed and dotted curves) incoming electrons/positrons and maximal top squark mixing. The photon contribution (dot-dashed curve) is suppressed by more than two orders of magnitude.

is expected for gluino masses of 540 (1004) GeV [6, 7]. If the masses and mixing angle(s) of the top (and bottom) squarks are known, a precision of $\pm 5 \dots 10$ GeV can be achieved at DESY TESLA for $m_{\tilde{g}} = 200$ GeV and maximal top squark mixing with an integrated luminosity of 100 fb^{-1} per center-of-mass energy point.

A center-of-mass energy scan for the scenario with no squark mixing, but large left-/right-handed squark splitting (case I) is shown in Fig. 9 for light (full and dashed curves) and heavy (dotted and dot-dashed curves) gluino masses. Since the photon contributes now significantly to the cross section, it proves to be advantageous to choose the lepton

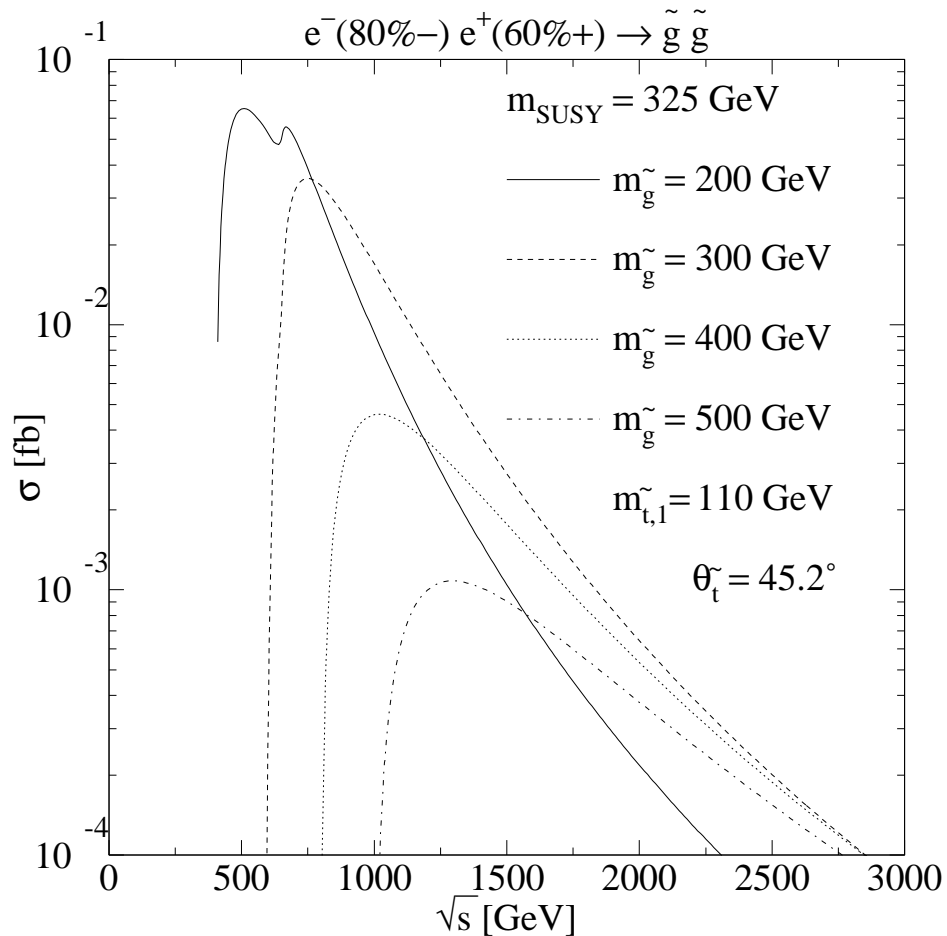


FIG. 7: Center-of-mass energy dependence of the polarized $e^+e^- \rightarrow \tilde{g}\tilde{g}$ cross section for various gluino masses and maximal top squark mixing.

polarization such that the Z^0 -boson interferes constructively with the photon, even though it is by itself slightly smaller than for the opposite choice. Since all three generations add now to the cross section, it can become almost an order of magnitude larger than in the mixing scenario (case II), and even gluino masses of 1 TeV may be observable at a multi-TeV collider like CERN CLIC. However, also here the cross section drops sharply when the squark mass splitting is reduced from 1500 TeV (full and dotted curves) to values close to m_{SUSY} (dashed and dot-dashed curves).

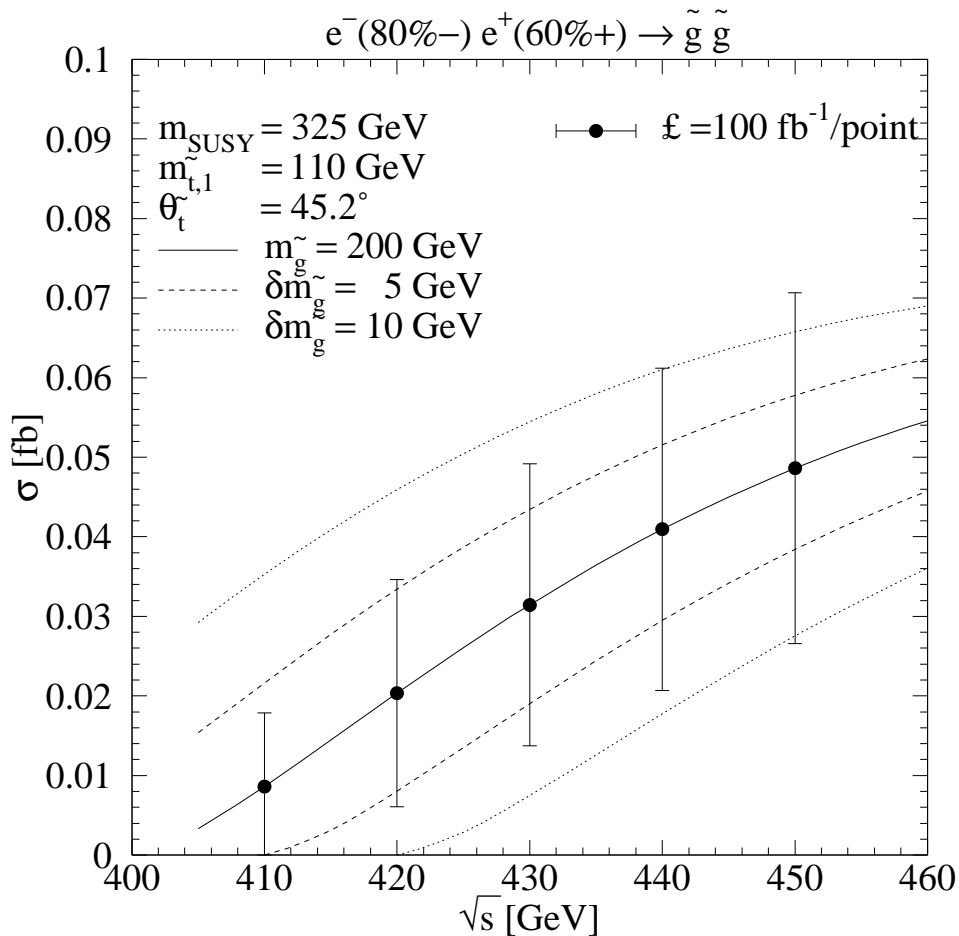


FIG. 8: Sensitivity of the polarized $e^+e^- \rightarrow \tilde{g}\tilde{g}$ cross section to the gluino mass $m_{\tilde{g}}$ for maximal top squark mixing. The central values and statistical error bars of the data points have been calculated assuming $m_{\tilde{g}} = 200 \text{ GeV}$ and a luminosity of 100 fb^{-1} per center-of-mass energy point.

IV. CONCLUSIONS

The purpose of this Paper has been two-fold: First, we have resolved a long-standing discrepancy in the literature about the relative sign of the quark and squark loop contributions to the production of gluino pairs in e^+e^- annihilation. We confirm the result of two older papers that the divergence cancels for each squark flavor separately and not between weak isospin partners [16, 17] and trace the sign problem in one case to the Feynman rules employed in the corresponding calculation [18]. Our results rely on two completely independent analytical calculations and one computer algebra calculation.

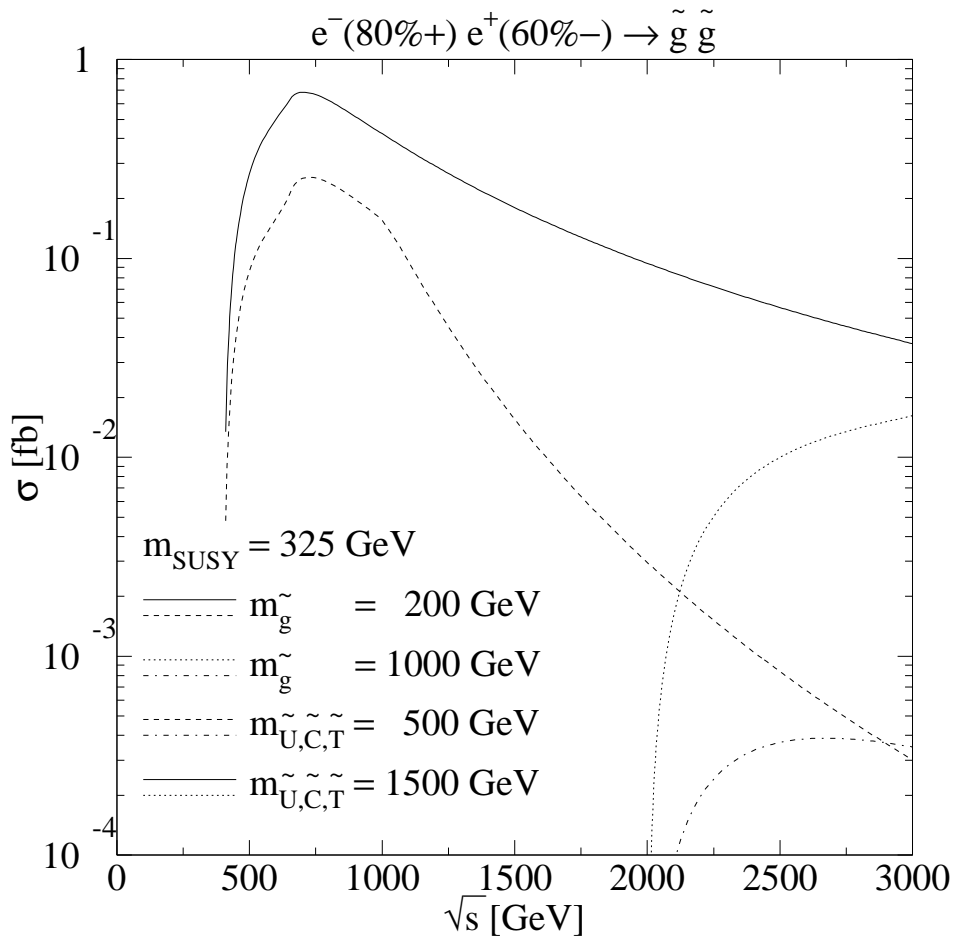


FIG. 9: Center-of-mass energy dependence of the polarized $e^+e^- \rightarrow \tilde{g}\tilde{g}$ cross section for various gluino masses and mass splittings between left- and right-handed up-type squarks.

Second, we have investigated the prospects for precision measurements of gluino properties, such as its mass or its Majorana fermion nature, at future linear e^+e^- colliders. We have taken into account realistic beam polarization effects, photon and Z^0 -boson exchange, and current mass exclusion limits. Previously, only light gluinos at center-of-mass energies up to the Z^0 -boson mass had been investigated. Within the general framework of the MSSM, we have concentrated on two scenarios of large left-/right-handed up-type squark mass splitting and large top squark mixing, which produce promisingly large cross sections for gluino masses up to 500 GeV or even 1 TeV. Gluino masses of 200 GeV can then be measured with a precision of about 5 GeV in center-of-mass energy scans with luminosities of $100 \text{ fb}^{-1}/\text{point}$. However, when both the left-/right-handed squark mass splitting and

the squark mixing remain small, gluino pair production in e^+e^- annihilation will be hard to observe, even with luminosities of $1000 \text{ fb}^{-1}/\text{year}$.

Acknowledgments

We thank B. Kileng, G. Kramer, and P. Osland for useful discussions and A. Brandenburg and B.A. Kniehl for a careful reading of the manuscript. This work has been supported by Deutsche Forschungsgemeinschaft through Grant No. KL 1266/1-2 and through Graduiertenkolleg *Zukünftige Entwicklungen in der Teilchenphysik*.

APPENDIX A: SQUARK MIXING

The (generally complex) soft SUSY-breaking terms A_q of the trilinear Higgs-squark-squark interaction and the (also generally complex) off-diagonal Higgs mass parameter μ in the MSSM Lagrangian induce mixings of the left- and right-handed squark eigenstates $\tilde{q}_{L,R}$ of the electroweak interaction into mass eigenstates $\tilde{q}_{1,2}$. The squark mass matrix [14, 35]

$$\mathcal{M}^2 = \begin{pmatrix} m_{LL}^2 + m_q^2 & m_q m_{LR}^* \\ m_q m_{LR} & m_{RR}^2 + m_q^2 \end{pmatrix} \quad (\text{A1})$$

with

$$m_{LL}^2 = (T_q^3 - e_q \sin^2 \theta_W) m_Z^2 \cos 2\beta + m_{\tilde{Q}}^2, \quad (\text{A2})$$

$$m_{RR}^2 = e_q \sin^2 \theta_W m_Z^2 \cos 2\beta + \begin{cases} m_{\tilde{U}}^2 & \text{for up - type squarks,} \\ m_{\tilde{D}}^2 & \text{for down - type squarks,} \end{cases} \quad (\text{A3})$$

$$m_{LR} = A_q - \mu^* \begin{cases} \cot \beta & \text{for up - type squarks} \\ \tan \beta & \text{for down - type squarks} \end{cases} \quad (\text{A4})$$

is diagonalized by a unitary matrix S , $S\mathcal{M}^2S^\dagger = \text{diag}(m_1^2, m_2^2)$, and has the squared mass eigenvalues

$$m_{1,2}^2 = m_q^2 + \frac{1}{2} \left(m_{LL}^2 + m_{RR}^2 \mp \sqrt{(m_{LL}^2 - m_{RR}^2)^2 + 4m_q^2 |m_{LR}|^2} \right). \quad (\text{A5})$$

For real values of m_{LR} , the squark mixing angle $\theta_{\tilde{q}}$, $0 \leq \theta_{\tilde{q}} \leq \pi/2$, in

$$S = \begin{pmatrix} \cos \theta_{\tilde{q}} & \sin \theta_{\tilde{q}} \\ -\sin \theta_{\tilde{q}} & \cos \theta_{\tilde{q}} \end{pmatrix} \quad \text{with} \quad \begin{pmatrix} \tilde{q}_1 \\ \tilde{q}_2 \end{pmatrix} = S \begin{pmatrix} \tilde{q}_L \\ \tilde{q}_R \end{pmatrix} \quad (\text{A6})$$

can be obtained from

$$\tan 2\theta_{\tilde{q}} = \frac{2m_q m_{LR}}{m_{LL}^2 - m_{RR}^2}. \quad (\text{A7})$$

If m_{LR} is complex, one may first choose a suitable phase rotation $\tilde{q}'_R = e^{i\phi}\tilde{q}_R$ to make the mass matrix real and then diagonalize it for \tilde{q}_L and \tilde{q}'_R . $\tan \beta = v_u/v_d$ is the (real) ratio of the vacuum expectation values of the two Higgs fields, which couple to the up- and down-type (s)quarks. The weak isospin quantum numbers for left-handed up- and down-type (s)quarks with hypercharge $Y_q = 1/3$ are $T_q^3 = \{+1/2, -1/2\}$, whereas $Y_q = \{4/3, -2/3\}$ and $T_q^3 = 0$ for right-handed (s)quarks, and their fractional electromagnetic charges are $e_q = T_q^3 + Y_q/2$. The soft SUSY-breaking mass terms for left- and right-handed squarks are $m_{\tilde{Q}}$ and $m_{\tilde{U}}, m_{\tilde{D}}$, respectively, and m_Z is the mass of the neutral electroweak gauge boson Z^0 .

APPENDIX B: FEYNMAN RULES

Denoting squark mass eigenstates by i, j, \dots , Lorentz indices by μ, ν, \dots , and color indices of the fundamental (adjoint) representation of the color symmetry group $SU(3)$ by l, m, \dots (a, b, \dots), we obtain the following propagators in Feynman-gauge:

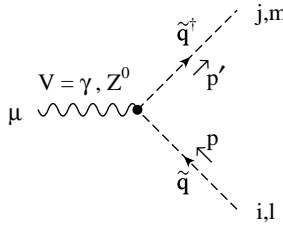
$$\begin{array}{c} \mu \bullet \text{---} \text{wavy line} \text{---} \bullet \nu \\ \text{V} = \gamma, Z^0 \\ \xrightarrow{\text{p}} \end{array} \quad \frac{-ig^{\mu\nu}}{p^2 - m_V^2 + i\eta}, \quad m_V^2 = \{0, m_Z^2\} \quad (\text{B1})$$

$$\begin{array}{c} l \bullet \text{---} \text{solid line} \text{---} \bullet m \\ \xrightarrow{\text{p}} \\ \text{q} \end{array} \quad \frac{i(\not{p} + m_q)\delta_{lm}}{p^2 - m_q^2 + i\eta} \quad (\text{B2})$$

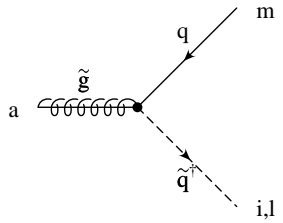
$$\begin{array}{c} i, l \bullet \text{---} \text{dashed line} \text{---} \bullet j, m \\ \xrightarrow{\text{p}} \\ \tilde{q} \end{array} \quad \frac{i\delta_{ij}\delta_{lm}}{p^2 - m_{\tilde{q}}^2 + i\eta} \quad (\text{B3})$$

Dirac fermions carry an arrow, which indicates the fermion number flow, whereas Majorana fermions, such as gluinos, do not carry arrows. An additional arrow is depicted next to all fermion lines in order to obtain a unique orientation of the fermion flow, which is evaluated according to the rules in [36]. The interaction vertices are given by [14]

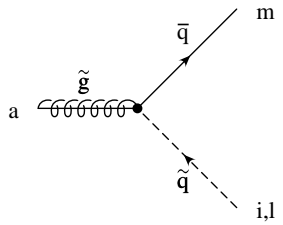
$$\begin{array}{c} \mu \text{---} \text{wavy line} \text{---} \bullet \\ \text{V} = \gamma, Z^0 \\ \begin{array}{l} \nearrow \text{f} \\ \searrow \bar{f} \end{array} \\ \text{m} \\ \text{l} \end{array} \quad -ie\gamma_\mu (v_f^V - a_f^V \gamma_5)\delta_{lm} \left\{ \begin{array}{l} v_f^\gamma = e_f \quad a_f^\gamma = 0 \\ v_f^Z = \frac{T_f^3 - 2e_f \sin^2 \theta_W}{2 \sin \theta_W \cos \theta_W} \quad a_f^Z = \frac{T_f^3}{2 \sin \theta_W \cos \theta_W} \end{array} \right. \quad (\text{B4})$$



$$-ie(p + p')_\mu \Gamma_q^{ij,V} \delta_{lm} \begin{cases} \Gamma_q^{ij,\gamma} = e_q \delta_{ij} \\ \Gamma_q^{ij,Z^0} = \frac{(T_q^3 - e_q \sin^2 \theta_W) S_{j1} S_{i1}^* - e_q \sin^2 \theta_W S_{j2} S_{i2}^*}{\sin \theta_W \cos \theta_W} \end{cases} \quad (\text{B5})$$



$$i\Gamma_{i,1}^a = -i\sqrt{2}\hat{g}_s T_{lm}^a (S_{i1} P_L - S_{i2} P_R) \quad (\text{B6})$$



$$i\Gamma_{i,2}^a = -i\sqrt{2}\hat{g}_s T_{ml}^a (S_{i1}^* P_R - S_{i2}^* P_L) \quad (\text{B7})$$

The Feynman rules in Eq. (B4) apply to photon and Z^0 -boson interactions with quarks and charged leptons. The latter carry electromagnetic charge $e_\ell = -1$ and weak isospin $T_\ell^3 = -1/2$ (left-handed) and 0 (right-handed), but no color ($\delta_{lm} \rightarrow 1$). The gauge couplings g and g' of the weak isospin and hypercharge symmetries $SU(2)_L$ and $U(1)_Y$ have been expressed in terms of the electromagnetic coupling $e = g \sin \theta_W$ and the sine and cosine of the weak mixing angle $\sin \theta_W / \cos \theta_W = g' / g$. The gluino-quark-squark vertices depend on the generators of the $SU(3)$ color symmetry group, T_{lm}^a , and on the Yukawa coupling \hat{g}_s , which is identical to the strong gauge coupling g_s in leading order, and on the squark mixing matrix S , but not on the orientation of the fermion flow.

[1] M. Carena *et al.*, arXiv:hep-ph/0010338.

[2] S. Abel *et al.*, arXiv:hep-ph/0003154.

[3] R. Culbertson *et al.*, arXiv:hep-ph/0008070.

- [4] S. Ambrosanio *et al.*, arXiv:hep-ph/0006162.
- [5] B. Allanach *et al.*, arXiv:hep-ph/9906224.
- [6] A. Airapetian *et al.* [ATLAS Collaboration], CERN-LHCC-99-15.
- [7] S. Abdullin *et al.* [CMS Collaboration], *J. Phys. G* **28**, 469 (2002).
- [8] W. Beenakker, R. Höpker, M. Spira and P. M. Zerwas, *Nucl. Phys. B* **492**, 51 (1997).
- [9] J. A. Aguilar-Saavedra *et al.*, arXiv:hep-ph/0106315.
- [10] B. A. Campbell, J. R. Ellis and S. Rudaz, *Nucl. Phys. B* **198**, 1 (1982).
- [11] D. H. Schiller and D. Wähner, *Nucl. Phys. B* **259**, 597 (1985).
- [12] A. Brandenburg, M. Maniatis and M. M. Weber, arXiv:hep-ph/0207278.
- [13] H. P. Nilles, *Phys. Rept.* **110**, 1 (1984).
- [14] H. E. Haber and G. L. Kane, *Phys. Rept.* **117**, 75 (1985).
- [15] P. Nelson and P. Osland, *Phys. Lett. B* **115**, 407 (1982).
- [16] G. L. Kane and W. B. Rolnick, *Nucl. Phys. B* **217**, 117 (1983).
- [17] B. A. Campbell, J. A. Scott and M. K. Sundaresan, *Phys. Lett. B* **126**, 376 (1983).
- [18] B. Kileng and P. Osland, *Z. Phys. C* **66**, 503 (1995).
- [19] A. Djouadi and M. Drees, *Phys. Rev. D* **51**, 4997 (1995).
- [20] A. Denner, *Fortsch. Phys.* **41**, 307 (1993).
- [21] G. Passarino and M. J. Veltman, *Nucl. Phys. B* **160**, 151 (1979).
- [22] S. T. Petcov, *Phys. Lett. B* **139**, 421 (1984).
- [23] B. Kileng and P. Osland, private communication.
- [24] T. Hahn and M. Perez-Victoria, *Comput. Phys. Commun.* **118**, 153 (1999).
- [25] G. J. van Oldenborgh, *Comput. Phys. Commun.* **66**, 1 (1991).
- [26] T. Hahn and C. Schappacher, *Comput. Phys. Commun.* **143**, 54 (2002).
- [27] K. Hagiwara *et al.* [Particle Data Group Collaboration], *Phys. Rev. D* **66**, 010001 (2002).
- [28] T. Affolder *et al.* [CDF Collaboration], *Phys. Rev. Lett.* **88**, 041801 (2002).
- [29] S. Abachi *et al.* [D0 Collaboration], *Phys. Rev. Lett.* **75**, 618 (1995).
- [30] M. Felcini, C. Tully *et al.* [LEP Higgs Working Group Collaboration], Note 2001-04, arXiv:hep-ex/0107030.
- [31] J. Abdallah *et al.* [LEP SUSY Working Group Collaboration], <http://lepsusy.web.cern.ch/lepsusy>.
- [32] R. Barbieri and L. Maiani, *Nucl. Phys. B* **224**, 32 (1983).

- [33] M. Drees and K. Hagiwara, *Phys. Rev. D* **42**, 1709 (1990).
- [34] P. H. Chankowski, A. Dabelstein, W. Hollik, W. M. Mosle, S. Pokorski and J. Rosiek, *Nucl. Phys. B* **417**, 101 (1994).
- [35] J. F. Gunion and H. E. Haber, *Nucl. Phys. B* **272**, 1 (1986) [Erratum-ibid. *B* **402**, 567 (1993)].
- [36] A. Denner, H. Eck, O. Hahn and J. Küblbeck, *Nucl. Phys. B* **387**, 467 (1992).